DEPARTMENT OF TRANSPORTATION

Estimation of Crossing Conflict at Signalized Intersection Using High-Resolution Traffic Data

Gary A. Davis, Principal Investigator
Department of Civil, Environmental, and Geo- Engineering
University of Minnesota

March 2017

Research Project
Final Report 2017-08

To request this document in an alternative format, such as braille or large print, call 651-366-4718 or 1-800-657-3774 (Greater Minnesota) or email your request to ADArequest.dot@state.mn.us. Please request at least one week in advance.

Technical Report Documentation Page

1. Report No. MN/RC 2017-08	2.	3. Recipients Accession No.	
4. Title and Subtitle Estimation of Crossing Conflict at Signalized Intersection Using High-Resolution Traffic Data		5. Report Date March 2017 6.	
7. Author(s) Henry X. Liu, Gary A. Davis, Shengyin Shen, Xuan Di, and Indrajit Chatterjee		8. Performing Organization Report No.	
9. Performing Organization Name and Address Department of Civil, Environmental, and Geo- Engineering University of Minnesota 500 Pillsbury Drive SE Minneapolis, MN 55455		10. Project/Task/Work Unit No. CTS #2015013 11. Contract (C) or Grant (G) No. (c) 99008 (wo) 155	
12. Sponsoring Organization Name and Address Minnesota Department of Transportation Research Services & Library 395 John Ireland Boulevard, MS 330 St. Paul, Minnesota 55155-1899		13. Type of Report and Period Covered Final Report 14. Sponsoring Agency Code	
15. Supplementary Notes http:// mndot.gov/research/reports/2017/201708.pdf			
16. Abstract (Limit: 250 words) This project explores the possibility of using high-resolution traffic signal data to evaluate intersection safety. Traditional methods using historical crash data collected from infrequently and randomly occurring vehicle collisions can require several years to identify potentially risky situations. By contrast, the proposed method estimates potential traffic conflicts using high-resolution traffic signal data collected from the SMART-Signal system. The potential conflicts estimated in this research include both red-light running events, when stop-bar detectors are available, and crossing (i.e. right-angle) conflicts. Preliminary testing based on limited data showed that estimated conflict frequencies were better than AADT for predicting frequencies of angle crashes. With additional validation this could provide a low-cost and easy-to-use tool for traffic engineers to evaluate traffic safety performance at signalized intersections.			
17. Document Analysis/Descriptors Red light running, Signalized intersections, Traffic safety, Traffic conflicts, Right angle crashes, Traffic data		18. Availability Statement No restrictions. Document available from: National Technical Information Services, Alexandria, Virginia 22312	
19. Security Class (this report) Unclassified	20. Security Class (this page) Unclassified	21. No. of Pages 56	22. Price

Estimation of Crossing Conflict at Signalized Intersection Using High-Resolution Traffic Data

FINAL REPORT

Prepared by:

Henry X. Liu[1]
Gary A. Davis[2]
Shengyin Shen[1]
Xuan Di[1]
Indrajit Chatterjee[2]

1. Department of Civil and Environmental Engineering, University of Michigan
2. Department of Civil, Environmental, and Geo- Engineering, University of Minnesota

March 2017

Published by:

Minnesota Department of Transportation
Research Services & Library
395 John Ireland Boulevard, MS 330
St. Paul, Minnesota 55155-1899

ACKNOWLEDGMENTS

This work was supported by the MnDOT. The authors would like to thank Steve Misgen from MnDOT for his assistance in the field deployment of the SMART-Signal system. Jingru Gao assisted with preparation of the final report.

TABLE OF CONTENTS

LIST OF TABLES

LIST OF FIGURES

EXECUTIVE SUMMARY

Intersection safety has always been a critical concern to traffic engineers. Right-angle crashes are particularly important in intersection safety since they often involve severe crashes at signalized intersections. Traditionally, the number of crashes is a direct measure of intersection safety. However, crashes are rare events and it can take one or more years to collect sufficient data for safety assessment. Therefore, traditional methods, either using historical crash data collected from infrequent and random vehicle collisions or potential traffic conflicts estimated from a microscopic traffic simulators, which generally assume accident-free conditions, cannot provide evaluations of intersection safety that are both accurate and timely.

This project explores the possibility of using high-resolution traffic signal data, which can be directly collected from existing loop detector systems, to evaluate intersection safety. In this project, we developed a method to estimate potential traffic conflicts using high-resolution traffic signal data collected from the SMART-Signal system, which has been deployed at over 100 intersections in the Twin Cities. The potential conflicts estimated in this research include both red-light running events, when stop-bar detectors are available, and crossing (i.e., right-angle) conflicts. With the estimated conflicts, a regression model was developed to determine if adding a measure of crossing conflict to a more standard model containing annual average daily traffic (AADTs) could improve the ability to predict angle crashes at signalized intersections. Limited testing showed that estimated conflict frequencies were better than AADT for predicting frequencies of angle crashes. With additional validation this could provide a low-cost and easy-to-use tool for traffic engineers to evaluate traffic safety performance at signalized intersections.

CHAPTER 1: INTRODUCTION

About one million collisions occur at signalized intersections in the U.S. each year (Retting et al., 1998). Thus, intersection safety becomes a critical concern to traffic engineers.

Right angle crashes are very important in the intersection safety, because they are more likely to involve severe crashes at signalized intersections. Based on the data in a study conducted in the state of Florida (Abdel-Aty et al., 2005), it was found that around 45% of right-angle crashes involve injury whereas only around 25% of other crashes involve injury. The number of crashes is a direct measure of intersection safety. However, they are fortunately rare events and it thus takes a long time to collect sufficient data for safety assessment. For example, Mitra et al. (2002) studied the frequency of right angle crash using 52 four-legged signalized intersections in Singapore over 8 years (1992-1999). Poch and Mannering (1996) fit an angle crash frequency model for 63 four-legged intersections over 7 years (1987-1993).

Since the traditional method of evaluating the intersection safety relies heavily upon crash data, researchers have proposed surrogate methods to assess intersection safety as an alternative to crash data. Perkins and Harris (1967, 1968) first proposed the concept of traffic conflict and it was defined by Amundson and Hyden (1977) as “an observed situation in which two or more road users approach each other in space and time to such an extent that there is a risk of collision if their movement remains unchanged.” Conflicts occur much more frequently than actual collisions, and therefore have significantly greater sample sizes than do crash counts. This can make it easier and less costly to analyze safety-related characteristics of roadway segments and intersections. Therefore, traffic conflicts have become surrogate safety measures in the literature.

2.1 RESEARCH OBJECTIVES

The goal of this research was to explore the possibility of using high-resolution traffic signal data to evaluate intersection safety. The proposed method estimates potential traffic conflicts using high-resolution traffic signal data collected from the SMART-Signal system, which has been deployed at over 100 intersections in the Twin Cities area. The potential conflicts estimated in this research include both red-light running events, when stop-bar detectors are available, and crossing (i.e. right-angle) conflicts. Using the estimated traffic conflicts and the field collected crash occurrence data, a crash prediction model was evaluated.

2.2 BACKGROUND AND RELEVANT WORK

2.2.1 RLR Behavior Modeling

Driving behavior at intersections contributes significantly to intersection safety. When drivers encounter the onset of yellow, they choose to either stop or go. The stopping probability curve is needed to model drivers’ behavior and discrete choice models are commonly used. Gazis et al. (1960) analytically derived stopping probability curves using logistic regression and discussed various scenarios with different

approaching speeds. Sheffi and Mahmassani (1981) were the first to propose a probit model to characterize the stopping probability curve. Assume a driver only stops if the time to reach the stop bar is larger than a critical time t_{cr}: $P(stop) = P(t > t_{cr})$, where $P(stop)$ is the probability of stopping and the critical time t_{cr} is normally distributed due to driver variability. Various factors can contribute to t_{cr}, thus this term alone cannot sufficiently describe drivers' complex stop or go behavior. More generally, drivers' stop or go decision can be modeled as:

$$P(\text{stop}) = f(\sum_i \beta_i X_i) \quad (1)$$

where β are parameters and x_i are predictor variables.

The function can be specified in two ways: (1) logistic regression, where $f(\sum_i \beta_i X_i) = \frac{e^{\sum_i \beta_i X_i}}{1-e^{\sum_i \beta_i X_i}}$; and (2) probit regression, where $f(\sum_i \beta_i X_i)$ is the cumulative density function of a normal distribution.

2.2.2 Crossing Conflicts

In the literature, crossing conflicts can be estimated either through video data analysis or by simulation. Since video data analysis is usually time consuming, microscopic traffic simulation has been used for conflict estimation. Sayed et al. *(1994)* focused on the crossing conflicts at un-signalized intersection by using a computer simulation model called Traffic Safety Conflict Simulation (TSC-Sim). The model was validated by trained observers. Another simulation study on the crossing conflict was conducted by Archer (2005), Archer and Young (2010). They developed a gap acceptance model for un-signalized T and four leg intersections and applied this model in VISSIM to calculate the number and severity of conflicts. The model was calibrated and validated using video data. Gettman and Head (*2003)* developed the Surrogate Safety Assessment Model (SSAM) to conduct conflicts analysis using commercial microscopic traffic simulation software like VISSIM, AIMSUN and PARAMICS. Three types of the conflicts were included in their study: rear-end conflicts, crossing conflicts and lane changing conflicts.

In this research, we take advantage of the rich data collected from the SMART-SIGNAL system to develop a cost-effective way of predicting crossing conflicts. At a signalized intersection, red light running may incur crossing conflicts, which in turn can lead to right-angle crashes. Some researchers used the post encroachment times (PET) as a surrogate of the right angle crash (Gettman and Head 2003). Songchitruksa and Tarko (*2006*) indicated a potential relationship between PET distributions and right-angle crashes using 8 hours of video to capture PET and a regression model between total right angle crashes and crossing conflicts.

2.2.3 Data Collection Methods

To predict drivers' behavior while approaching intersections, a variety of data collections methods have been employed in existing literature. **Table 1.** 1 summarizes all data collection methods used in the existing literature. Each method's advantages and disadvantages are also given.

Table 1. 1 Data collection methods comparison

Method	Data collected	Advantage	Disadvantage	Reference
Video camera	Last-to-go: distance from stop line at the onset of yellow, travel time to stop bar from the onset of yellow. First-to-stop: distance from stop line at the onset of yellow, break-response time from onset of yellow to braking, time required to stop after braking. For all: approaching speed at the onset of yellow, time headway, tailway, action of vehicles in adjacent lanes less than 2s ahead, presence of vehicles/bicycles/pedestrians waiting on the side street, presence of opposing vehicles waiting to turn left, flow rate, cycle length, vehicle type	detailed information for each vehicle	limited time period of data collection, time-consuming video processing	Gates et al. (2007), Retting et al. (2008), Elmitiny et al. (2010), Papaioannou (2007), Sharma et al. (2011), Liu et al. (2007)
Observers	Observed: time the light changed to green, light status when the last vehicle crossed the intersection (only those entering on yellow or red), safety-belt use, direction, vehicle type. Estimated: gender, age, ethnic group, model year	cheap, flexible	limited time period of data collection, time-consuming video processing	Porter and England (2000)
Survey	Demographic information: age, educational level, occupation, parental status. Driving facts: e.g., previous involvement in red-light-running, previous	cheap, flexible, drivers' information is available	time-consuming to train those who conducts	Porter and Berry (2001),

	receipt of a traffic ticket for red-light-running and so on. Behavioral information: believing red-light-running to be a problem or dangerous, degree of frustration when driving on urban roads, contributing factors of stop-or-go behavior. Environment: residential city size.		survey, no real-time traffic data	Abbas et al. (2014)
High-resolution detection (SMART-SIGNAL)	Measured (from the advance detector): occupancy time (i.e., speed), time gap, traffic signal phase, presence of running vehicles in adjacent lanes. Estimated: TTI, approaching speed at the onset of yellow, distance-to-stop-bar at the onset of yellow	continuously monitored	no drivers' information, limited data type only for point locations	Chatterjee and Davis (2011), Wu et al. (2013), Lu et al. (2015)
Discrete point sensors	Measured: speed passing point detectors, acceleration rates between two point detectors. Estimated: acceleration	continuously monitored, acceleration is available by using averages of multiple sensors' speed information	no drivers' information, limited data type only for point locations	Zhang et al. (2009)
Advanced yellow-phase trigger	vehicles' trajectories, signal phase, time remaining in the yellow phase, distance-to-stop-bar to trigger the yellow phase, percent of brake application, percent of throttle application	in a controlled environment where various values of distance-to-stop-bar to trigger the yellow phase are set by researchers, and	limited samples, behavior may be artificial due to controlled environment	Rakha et al. (2007)

		drivers' detailed reactions (such as brake and throttle applications) can be measured		
Red light photo enforcement cameras	intersection where the violation occurred, data and time of the violation, age, gender, vehicle make and year of the vehicle driven by the violator, vehicle speed at the time of violation, elapsed time when crossing intersection after the onset of red	drivers' and vehicles' information are available	only information related to violators are available	Bonneson and Son, (2003), Retting et al. (2008), Yang and Najm (2007)

Compared to the traditional data collection methods for evaluating intersection safety, high-resolution traffic detector and signal phase data can be used to evaluate long-term intersection safety performance. To date there only exist three papers on utilizing high-resolution data to evaluate intersection safety. Chatterjee and Davis (2011) identified the changing points of occupancy data at the advance detector to infer right-angle crash occurrence. Wu et al. (2013) modeled drivers' stop-or-go behavior using information extracted from the advance detector. However, they did not distinguish whether or not the drivers' behavior happened in a dilemma zone and so blurred responsibilities of involved parties in a crash. For instance, a driver might run a red light from a dilemma zone because of a poorly designed traffic signal phase (which should be the traffic engineers' responsibility). But another case of red-light-running when sufficient stopping distance is available could result from aggressiveness (which should blame the driver). As the reasons for stop-or-go behavior in or outside a dilemma zone may be quite different, one model may not capture such variations. As an extension, Lu et al. (2015) further categorized 30,000 yellow-light-running cases into "in should-go zone", "in should-stop zone", "in dilemma zone", and "in option zone". The factors contributing to yellow-light-running behavior in each zone were analyzed. In this study, the dilemma or option zone was characterized by a set of fixed parameter values, such as the driver reaction time and acceleration or deceleration rate. These values may vary substantially among drivers and vehicles, however. As revealed by Liu et al. (2007) the dilemma zone locations vary among different groups of drivers and are thus dynamic, the division of the aforementioned into four zones based on fixed parameters can be highly questionable. Though the number of studies using high-resolution data is small, the existing literature shows that such datasets contain great potential for evaluating intersection safety performance.

2.3 ORGANIZATION OF THIS REPORT

The report is organized as follows. In chapter 2, we introduce the methodology for identifying red-light-running (RLR), first-to-stop (FSTP) and yellow-light-running (YLR) events for those intersections with both stop-bar detectors and entrance detectors. These were located along Trunk Highway (TH55) in Minnesota. As RLR events can cause conflicts and crashes, the relationship between traffic flow characteristics and RLR events are studied. Since most intersections along TH55 or TH13 contain neither stop-bar nor entrance detectors, in chapter 3 we develop a methodology of identifying crossing conflicts at intersections with advance detectors only. In chapter 4, the Poisson regression is used to link crossing conflicts and right-angle crashes. The volume-based model is also developed as a comparison. Conclusions are given in Chapter 5.

CHAPTER 2: IDENTIFYING FIRST-TO-STOP (FSTP), YELLOW-LIGHT RUNNING (YLR), AND RED-LIGHT-RUNNING (RLR) EVENTS USING STOP BAR AND ENTRANCE DETECTORS

In Chapter 2, we will introduce the methodology of identifying first-to-stop (FSTP), yellow-light-running (YLR), and red-light-running (RLR) events for those intersections with both stop bar detectors and entrance detectors located along TH55. As RLR events may cause conflict and crash, the relationship between traffic flow characteristics and RLR events will be further studied.

Before proceeding, notations which will be used in the rest of the report are listed as follows:

RLR: Red light running event;

YLR: Yellow light running event;

FSTP: First to stop event;

D_a: Advance detector;

D_s: Stopbar detector;

D_e: Entrance detector;

$T_{a/s/e}$: Timestamp of vehicle actuation at advance/ stop-bar /entrance detector;

$t_{a/s/e}$: Time headway at advance/stop-bar/entrance detector;

V_a: Vehicle speed at advance detector;

V_s: Vehicle speed at stopbar detector;

V_e: Vehicle speed at entrance detector;

l_{se}: Distance between the stop-bar detector and the entrance detector;

l_s: Distance between the stop-bar detector and the stop bar;

l_a: Distance between the advance detector and the stop bar;

L : Distance between the vehicle and the stop bar;

T_Y: Start timestamp of the yellow phase;

$Y_{a/s/e}$: Yellow light running event at advance/ stop-bar /entrance detector;

$R_{a/s/e}$: Red light running event at advance/ stop-bar /entrance detector;

$F_{a/s/e}$: First to stop event at advance/ stop-bar /entrance detector.

Red-light running can potentially cause crashes between vehicles coming from a major and a minor road, which can thus be used as a surrogate to evaluate intersection safety. Our first task is to identify these events using SMART-SIGNAL data.

For drivers who choose to stop, we are interested in those who are the first to stop during each cycle, called "first-to-stop" (FSTP). Those drivers who choose to go can be further divided into two types: cross during yellow phase (called "yellow-light-running" (YLR)) and cross during red phase (called "red-light-running" (RLR)). See **Figure 2.1** for classification of these three events. The abbreviations used in this report follow Wu et al. (2014). Along TH 55, several intersections are equipped with three detectors: advance detector, stop bar detector, and entrance detector. As stop bar detectors are located close to stop bar, using data from stop bar detector can identify each event to a high degree of accuracy. Combined with entrance detector, RLR can be further verified. In the following, we will use data collected from stop bar to identify FSTP, YLR, and RLR events and then use entrance detectors to verify them.

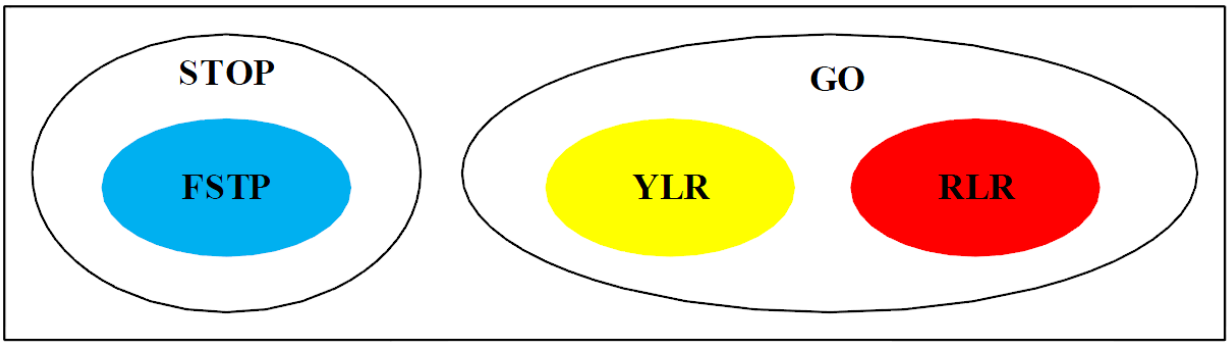

Figure 2.1 FSTP, YLR, and RLR events classification

2.4 METHODOLOGY

The methodologies of identifying these events will be discussed step by step in the rest of Chapter 2. The flowchart of the algorithm is illustrated in **Figure 2. 2**:

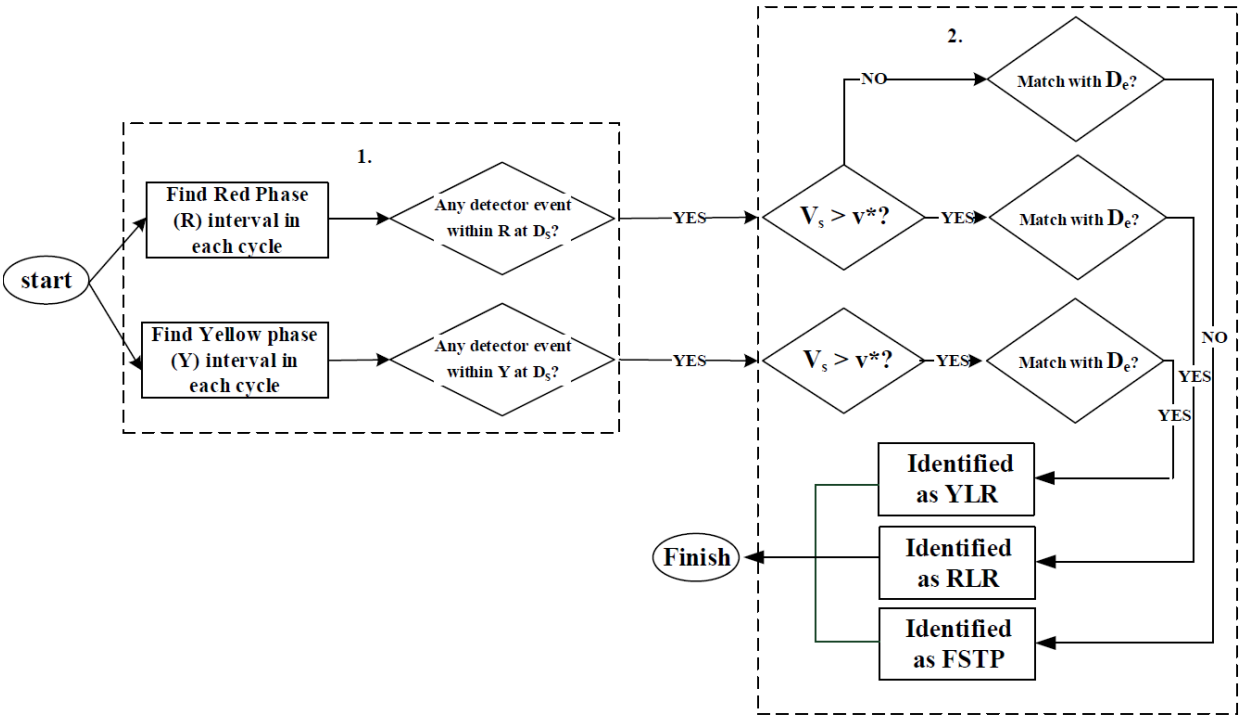

Figure 2. 2 Algorithm of RLR, YLR and FSTP identification

First, we obtain the start timestamp and duration of yellow and red phases of each cycle. Then all the events actuating the stop-bar detector during yellow and red signal phases will be extracted.

Second, among all events identified in the first step, FSTP/YLR/RLR will be selected using both stop bar and entrance detectors. The algorithm related to the second step is illustrated in **Figure 2. 3** and this figure will be revisited throughout the report.

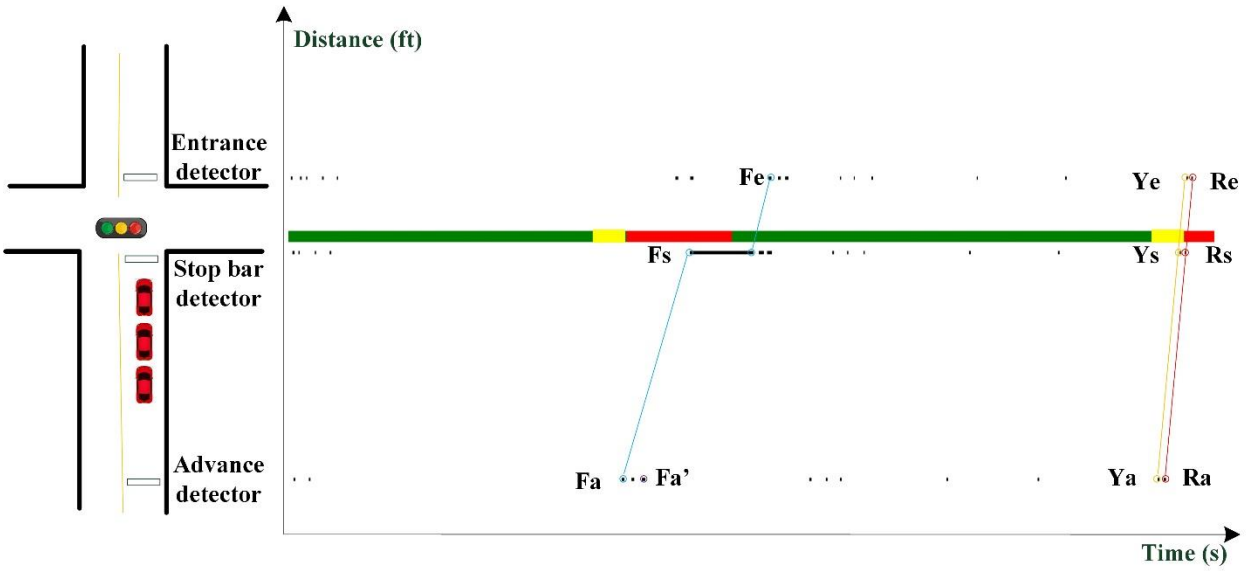

Figure 2. 3 SMART-SIGNAL data visualization in time-space diagram

Figure 2. 3 plots the data collected from the SMART-SIGNAL system. The left-hand diagram illustrates the detector layout of the SMART-SIGNAL system at a typical intersection of one major and one minor roads. The right-hand graph is the time-space diagram where the x-axis stands for timestamp and the y-axis for distance. The green/yellow/red bar in the middle indicates signal phase status, whose start timestamp and phase duration associated with each phase are extracted from the SMART-SIGNAL system. The black line represents a detector actuation event. Its start point shows the timestamp when one vehicle arrives at one detector and its length represents the occupancy of the vehicle on that detector.

In **Figure 2.** 3, event F indicates an FSTP case. It arrives at the stop-bar detector (indicated as F_s) after the signal phase turns to red and successfully stops before the stop bar. A long black line following the actuation event F_s indicates that a vehicle remains static on the stop-bar detector for a period of time until the signal turns to green. On the contrary, events Y and R represent "go" cases. "Go" vehicles arrive at the stop-bar detector (indicated as Y_s and R_s) during yellow or red and successfully pass the intersection. Accordingly, their actuations are two very short line segments because "go" vehicles usually approach intersections at a high speed. Based on this observation, we propose the following algorithm to identify "stop" and "go" events.

Assume all vehicles approach the intersection at the maximum deceleration rate $a^- = 10\ ft/s^2$ (the value is suggested by ITE). Given the stop-bar detector is usually located 40 to 60 feet upstream from the stop bar along TH55, if vehicles successfully come to a stop from the stop-bar detector to the stop bar, the maximum speed at the stop-bar detector should be: $v^* = \sqrt{2 * a^- * l_s}$, where a^- is the maximum deceleration rate and l_s is the distance from the stop-bar detector to the stop bar. If a vehicle's speed at the stop bar $V_a \leq v^*$, it is identified as a "stop" case; otherwise it is a "go" case. Among all the "go" events, those who pass the stop-bar detector during the yellow phase are identified as "YLR", during red phase are identified as "RLR".

To verify the identified RLR, YLR and FSTP events, we further use downstream entrance detectors located about $110\ ft$ downstream from the intersection. For a "go" event, we should be able to find another actuation at the entrance detector after a few seconds; otherwise, there should not exist any actuation until the signal turns to green. We assume that vehicles do not change lanes and keep a constant deceleration or acceleration rate traveling from the stop-bar detector to the entrance detector due to the sufficiently short distance between these two detectors. To match each actuation at the stop-bar doctor to the entrance detector, we propose the following matching algorithm which is similar to that proposed by Wu et al. (2013):

1. Assume the vehicle travels at a constant speed from the stop-bar detector to the entrance detector. The constant speed is calculated as the average speed between two detectors, i.e., $\bar{v} = \frac{v_s + v_e}{2}$.
2. A timestamp window for YLR/RLR vehicles to arrive at the entrance detector is computed as: $[T_s + \frac{l_{se}}{\bar{v}} - 2, T_s + \frac{l_{se}}{\bar{v}} + 2]$, where a buffer time of 2-second is added to accommodate variation. For FSTP, there should not exist any matching events at the entrance detector during the red phase. For YLR/RLR, the event(s) falling within the time window is/are identified as the right match. We should note that selection of 2-second is based on engineering judgement. A longer than 2-second buffer may result in multiple matches and a shorter than 2-second buffer may lead to no-match for most cases.
3. When multiple events are matched, we will further compare time headways with its leading vehicle at the stop-bar detector t_s and at the entrance detector t_e respectively across all matched pairs. The pair which has the closest headways at two detectors will be picked. Mathematically, $i^* = min_i \left| t_s - t_e^i \right|$, where i is the index of the potentially identified cases.

In Error! Reference source not found., there does not exist a match F_e at the entrance detector for F_s until after the signal phase turns to green. Cases Y_s, R_s are both matched to entrance actuations Y_e, R_e respectively. Therefore we can confirm that they are "go" events.

Among three events, RLR may potentially cause crossing conflicts and crash, so we will analyze its relationship with traffic flow characteristics at one intersection along TH55.

2.5 RLR EVENTS

The intersection Boone Ave/TH55 is chosen and its detector layout is shown in **Figure 2.4**. Detector No. 32, 31, 26, 27 are major road stop-bar detectors, located 60 feet upstream from the stop bar. Detector No. 28, 29, 33, 34 are entrance detectors, located 162 feet downstream from the stop bar. Detector No. 7, 8, 9, 10 are advance detectors, located 400 feet upstream from the stop bar. The data we use is extracted from 12/2008 to 09/2009.

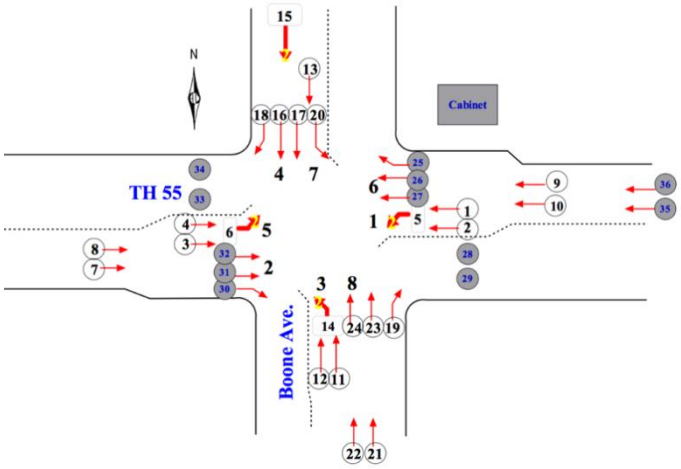

Figure 2.4 Intersection Boone/TH 55 layout

Figure 2. 5 plots the total number of RLR vs. the total traffic volume in each lane in each direction. It is apparent that the number of RLR in the eastbound is greater than that in the westbound in general. The reason is, most traffic travelling eastbound just gets off freeway at a higher speed and will thus have a higher tendency of running red light. On the other hand, vehicles traveling westbound primarily come from a few convective upstream signalized intersections at a lower speed, which can mitigate the RLR behavior. **Table 2.1** illustrates the average speed in each lane. It is not surprising that the average speed of vehicles travelling eastbound is greater than that travelling westbound.

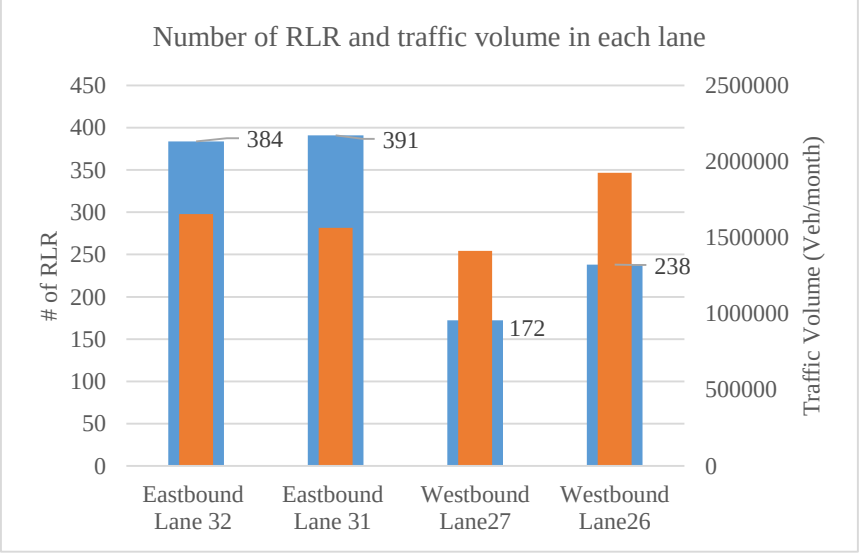

Figure 2. 5 Number of RLR vs. Traffic Volume (veh/month)

Table 2.1 Average speed in each lane

Intersection/Lane	Boone/32	Boone/31	Boone/26	Boone/27
RLR's speed at stop bar detector (ft/s)	82.6	74.7	58.8	68.2
Average speed at green phase at stop bar detector (ft/s)	52.9	51.15	40.44	46.2
Average speed at green phase at advance detector (ft/s)	68.7	67.1	55.7	65.4

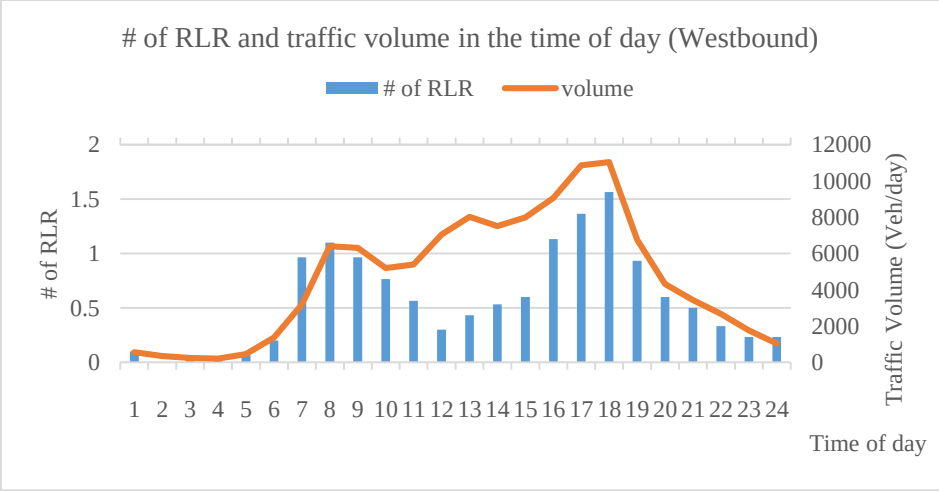

(a)

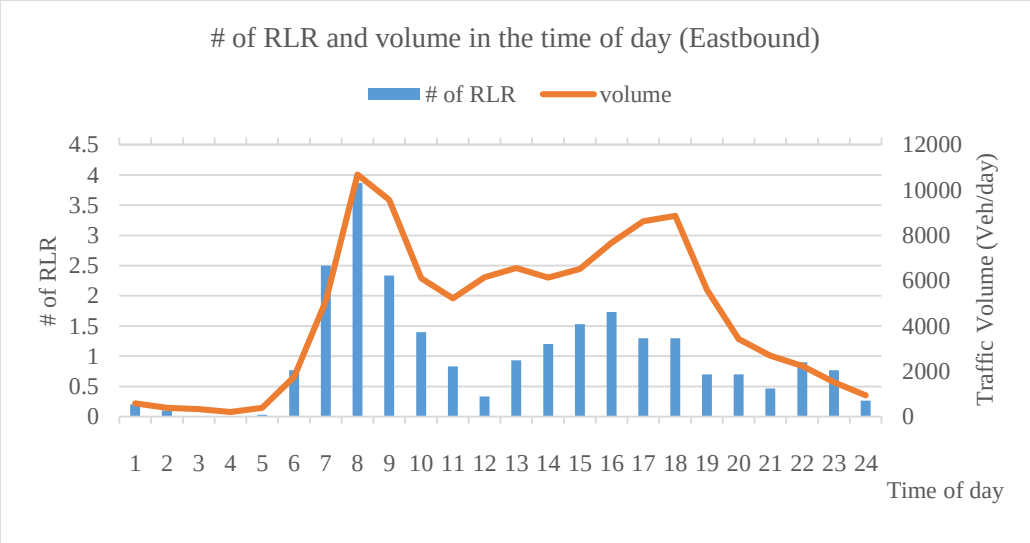

(b)

Figure 2. 6 Number of RLR vs. traffic volume over the time of day for (a) westbound and (b) eastbound

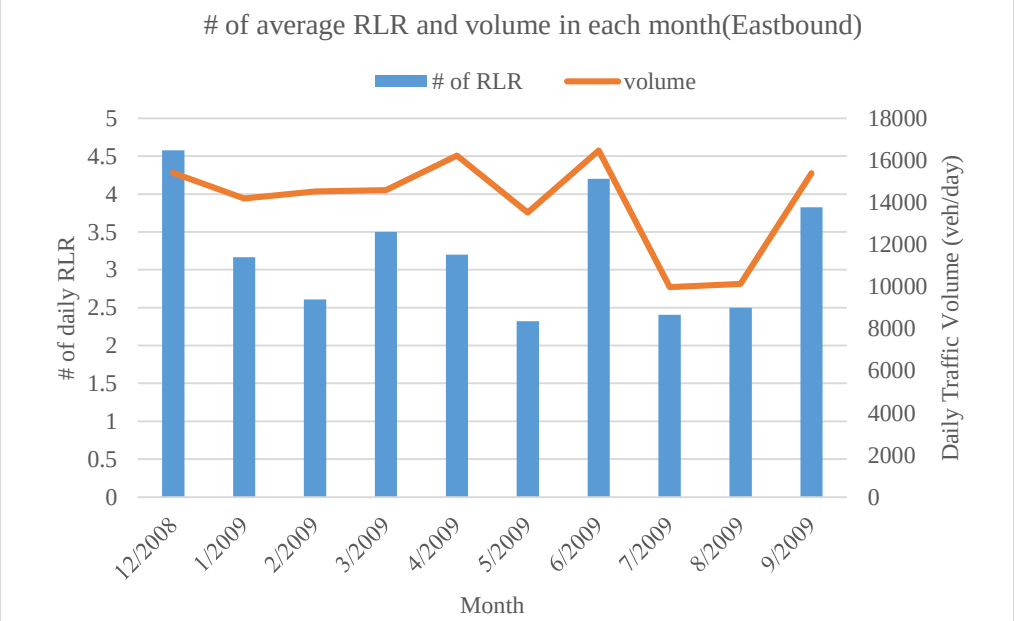

(a)

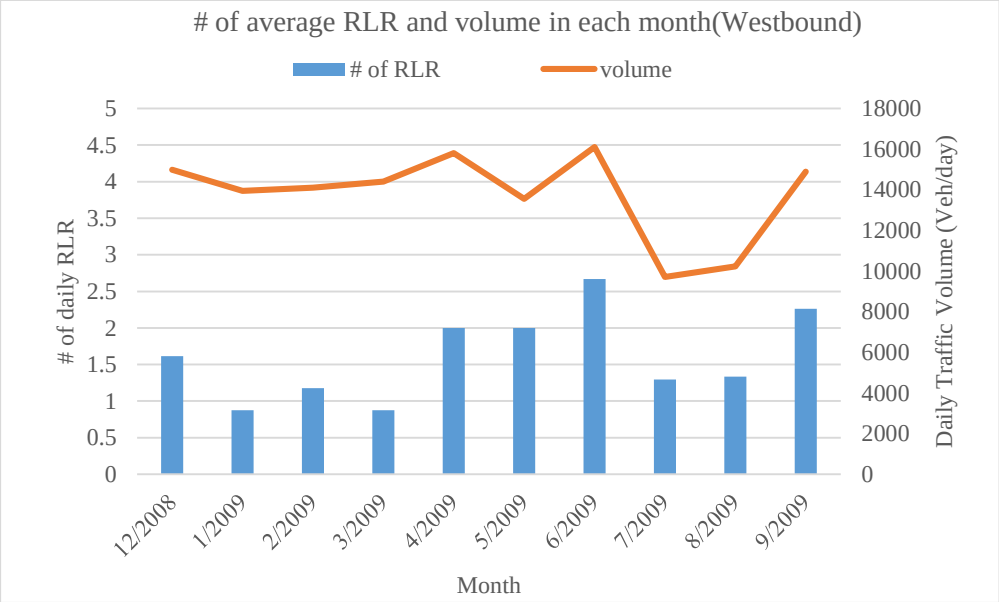

(b)

Figure 2. 7 Number of RLR vs. daily traffic volume in each month for (a) westbound and (b) eastbound

Figure 2. 6 and **Figure 2.** 7 further illustrate the average number of RLR vs. average traffic volume during the time of day and for each month, respectively. The magnitude of the number of RLR shows similar patterns as the average traffic volume in both cases.

2.6 MODELING STOP-OR-GO BEHAVIOR USING ADVANCE DETECTOR DATA

Ideally, RLR can be used as a surrogate to evaluate intersection safety. However, not all intersections are equipped with stop-bar detectors, which prevents us from accurately identifying RLR events. Therefore, we have to use another surrogate, i.e., crossing conflict, for the intersection safety evaluation purpose. As almost every intersection contains one advance detector, in this chapter, we will aim to develop a methodology of predicting drivers' stop-or-go behavior using only advance detector data. After "go" events are identified along both major and minor roads, we will be able to capture a crossing conflict.

To ensure that the developed model can capture those "go" events to a certain degree of accuracy, we will have to first focus on those intersections equipped with stop bar and entrance detectors, which will help train a model using the actual "go" events. Specifically, we will extract relevant information of all "go" and "stop" events (identified with the help of stop bar and entrance detectors) recorded at advance detectors. Then a statistical model will be trained using the available information. It will then be used for predicting "go" events at intersections where only advance detectors are equipped.

2.6.1 Matching Events to Advance Detectors and Data Extraction

After FSTP/YLR/RLR events are identified at the stop-bar detector and verified by the entrance detector, illustrated in Section 2.1, now we need to match them to the advance detector. Matching YLR/RLR events from the stop-bar detector to the advance detector is the same as matching them to the entrance detector. Matching FSTP events to the advance detector, however, is different from matching them to the entrance detector. If we use the same algorithm as introduced in Section 2.1, there will be mismatches. For example, in **Figure 2.** 3, while trying to find the match F_a for F_s, if a 2-second time-window is defined, event F_a' will be recognized as the match. However, the actual one is F_a. The trajectory connecting F_a and F_s is not as steep as that connecting F_a' and F_s, meaning the vehicle is actually decelerating. The reason for mismatching is that the traffic dynamic between the advance detector and the stop-bar detector spanning 400 feet is complicated during the yellow phase due to queuing built-up. In addition, stopping vehicles' deceleration manifests great variations in terms of when and where to start to decelerate and where to stop. We found out that such mismatches are quite common for FSTP events and can further impair the subsequent analysis. Therefore, to match FSTP cases to the advance detector more accurately, we will match the last "go" event (i.e., the vehicle right in front of the FSTP). Because "go" vehicles usually keep relatively constant speed or accelerate rate and do not show significant variation in speed compared to stopping vehicles. After the last "go" event is matched, FSTP is the one following the matched "go" event.

The information extracted from the advance detector can be divided into two types: direct information and derived information (e.g., speed and distance-to-stop bar at the onset of yellow phase). **Table 2. 2** lists all information directly extracted from the advance detector.

Table 2. 2 Direct information extracted from the advance detector

$SignalPhase$	The signal phase status when the vehicle actuates the advance detector (s)
$Speed$	The speed of the vehicle, calculated as the effective vehicle length divided by occupancy (the effective vehicle length is suggested by ITE as 25 ft) (ft/s)
$Headway$	The time headway with the leading vehicle, computed as the difference between two events' actuation timestamp (s)
Occ_{max}	the maximum occupancy time during one cycle (s)
$Traffic\ Volume$	The traffic volume in one cycle, calculated as the number of vehicles passing by the advance detector in each cycle divided by the cycle length (veh/h). Along TH 55, the cycle length is fixed to 180s during the morning peak hour but it may vary based on the time of day
$Hour$	The hour when the actuation happens, extracted from the event actuation timestamp in the event data (h)

$Oversaturation$	Oversaturation happens when there exists any actuation whose occupancy at the advance detector is longer than 3s within the past two consecutive cycles
$LongVeh$	Whether each vehicle is a long vehicle is identified by the algorithm of length-based vehicle classification proposed in (Liu and Sun 2014)
Occ_1	The first leading vehicle's occupancy (s)
Occ_2	The second leading vehicle's occupancy (s)
Occ_3	The third leading vehicle's occupancy (s)

To derive vehicles' speed and distance-to-stop bar at the onset of yellow phase, we need to discuss three cases regarding the signal phase status when a vehicle arrives at the advance detector.

Assume that: (1) vehicles run at a constant speed from the advance detector to the onset of yellow phase (corresponding to Case 1) and (2) vehicles run at a constant speed from the onset of yellow phase to the advance detector (corresponding to Case 2 and 3). Given these two assumptions, speed at the onset of yellow is assumed to carry the same value measured at the advance detector, i.e., v_a. Note that the second assumption may not be reasonable because if one vehicle sees yellow phase and decides to stop, it tends to slow down. However, as the distance from the advance detector to stop bar is 400 feet, we assume that "stopping" vehicles may not decelerate so much at a sufficiently far distance.

Case 1: the signal phase is green when the vehicle arrives at the advance detector:

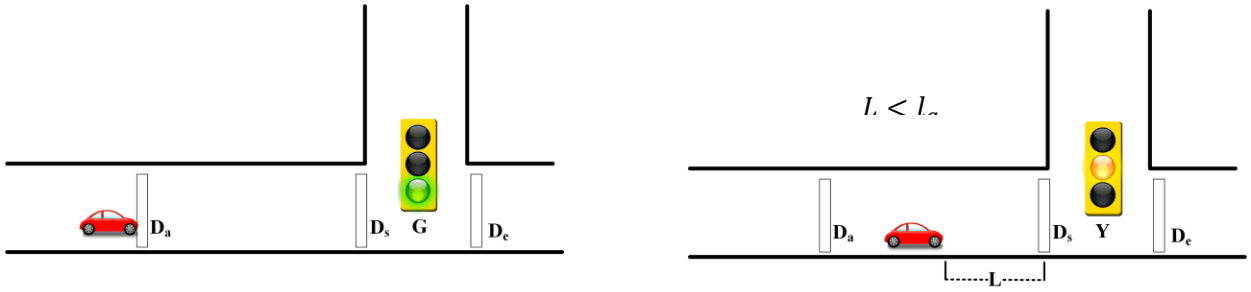

Case 2: the signal phase is yellow when the vehicle arrives at the advance detector:

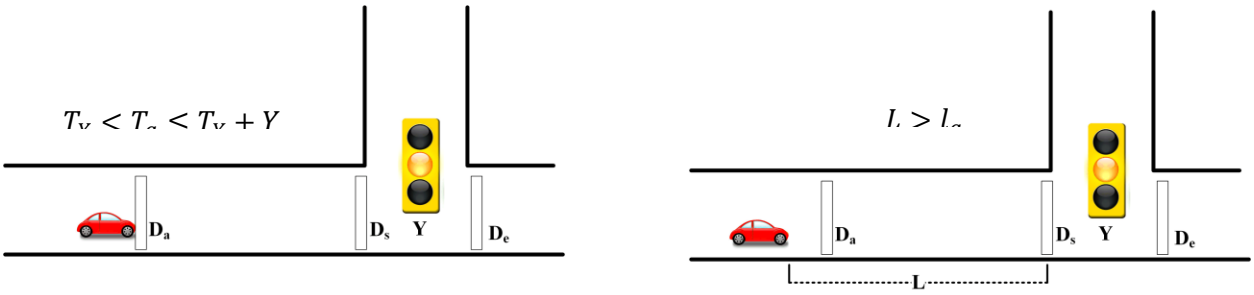

Case 3: the signal phase is red when the vehicle arrives at the advance detector:

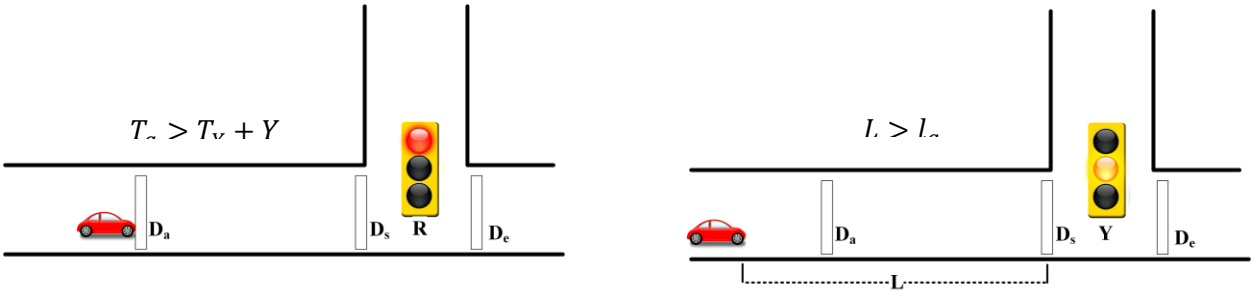

Figure 2. 8 Three scenarios when a vehicle arrives at the advance detector

Define

$$Phase\ status = T_a - T_Y = \begin{cases} < 0, if\ arrives\ at\ the\ D_a.during\ green\ , \\ = 0, if\ arrives\ at\ the\ D_a\ at\ the\ onset\ of\ yellow\ phase, \\ \in (0, Y], if\ arrives\ at\ the D_a\ during\ yellow\ phase, \\ > Y, if\ arrives\ at\ the\ D_a\ during\ red\ phase. \end{cases} \quad (2)$$

The distance-to-stop-bar L at the onset of yellow phase can thus be estimated as:

$$L = L_a + p * v_a. \quad (3)$$

Time-to-intersection (TTI) is defined as the time one vehicle takes to reach the intersection from the onset of yellow phase. It is computed as:

$$TTI = \frac{L}{v_a}. \quad (4)$$

From the SMART-SIGNAL system, we extract RLR/YLR/FSTP events using the algorithm proposed in Section 2. The parameters associated to each event, such as distance to the stop bar at the onset of yellow phase, speed, are directly or indirectly extracted from the advance detector.

We will now use the intersection Rhode Island/TH55 to illustrate how high-resolution data can help identify dilemma/option zone boundaries. The reason we pick this intersection is that it contains three legs, i.e., there exists no right-turn. Accordingly, the proposed matching algorithm will work more

accurately and events mismatch will be unlikely to happen. The link between two intersections is 752 ft long and its speed limit is 55mi/h. The detector deployment layout is shown in **Figure 2.** 9. Detector No. 16, 17, 13, 12 are stop-bar detectors, located on the main road 10 feet upstream from the stop bar. Detector No. 14, 15, 18, 19 are entrance detectors, deployed 142 feet downstream from the stop bar. Detector No. 1, 2, 9, 10 are advance detectors, located 375 feet upstream from the stop bar.

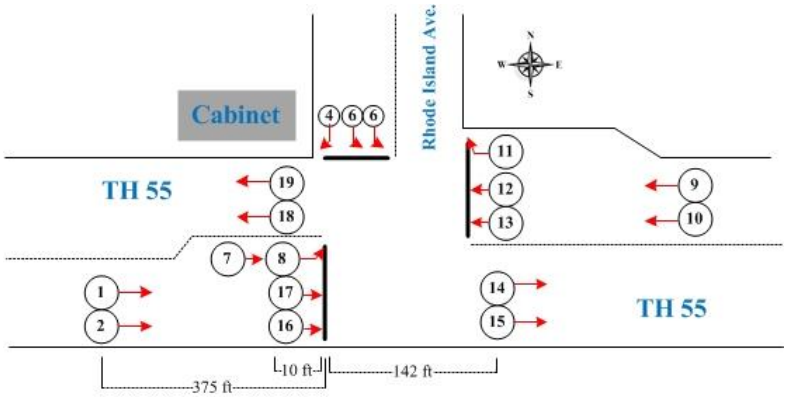

Figure 2. 9 Intersection Rhode Island/TH 55 layout

Table 2. 3 shows the detailed description of the data we use at intersection Rhode Island/TH55 to model and predict stop-or-go behavior.

Table 2. 3 Description of datasets at Rhode Island/TH55 intersection

	Time period	**RLR events**	**YLR events**	**FSTP events**
Training dataset	Nov. May. Jul.	228	8454	7575
Training dataset within dilemma or option zone	Nov. May. Jul.	122	3905	1335
Validation dataset	Aug. Sep.	82	3555	2994
Validation dataset within dilemma or option zone	Aug. Sep.	43	1632	520

We choose not to use the data from the month of December to April to remove the snow effects. Data of June 2009 is incomplete, so it is also excluded from the analysis.

2.6.2 Training a Stop-Or-Go Model

The logistic regression is used to model drivers' stop-or-go behavior in face of yellow with the extracted information from the advance detector (listed in **Table 2. 2**):

$$\log(\frac{P(go)}{P(stop)}) = \beta_0 + \beta_1 SignalPhase + \beta_2 Speed + \beta_3 Headway + \beta_4 \log(Occ_{max}) + \beta_5 Flow + \beta_6 Hour + \beta_7 Oversaturation + \beta_8 LongVeh + \beta_9 \log(Occ_1) + \beta_{10} \log(Occ_2) + \beta_{11} \log(Occ_3) \quad (5)$$

The estimated coefficients of logistic regression are listed in **Table 2. 4.**

Table 2. 4 Coefficients of logistic regression

Coefficients	Estimate	Std. Error	Z value	Pr(>|z|)
(Intercept)	-2.748e+00	1.343e+00	-2.047	0.0407 *
Signal Phase	-1.451e+00	5.181e-02	-28.007	<2e-16 ***
Speed	8.024e-02	5.417e-03	14.812	<2e-16 ***
Headway	-1.537e-02	2.467e-03	-6.230	4.68e-10 ***
Occ_{max}	-5.297e-01	1.310e-01	-4.043	5.28e-05 ***
Traffic Volume	4.030e-04	1.871e-04	2.154	0.0313 *
1:00 am	-1.415e+01	3.247e+02	-0.044	0.9652
2:00 am	-1.267e+01	3.247e+02	-0.039	0.9689
4:00 am	2.627e+01	2.520e+03	0.010	0.9917
5:00 am	-1.347e+00	1.397e+00	-0.964	0.3349
6:00 am	-1.358e+00	1.291e+00	-1.051	0.2931
7:00 am	-1.818e+00	1.296e+00	-1.403	0.1606
8:00 am	-1.316e+00	1.309e+00	-1.006	0.3144
9:00 am	-1.838e+00	1.281e+00	-1.435	0.1514

10:00 am	-1.881e+00	1.278e+00	-1.472	0.1410
11:00 am	-2.207e+00	1.275e+00	-1.730	0.0836 .
12:00 pm	-2.271e+00	1.275e+00	-1.781	0.0750 .
13:00 pm	-2.582e+00	1.275e+00	-2.025	0.0429 *
14:00 pm	-2.082e+00	1.279e+00	-1.629	0.1034
15:00 pm	-1.897e+00	1.281e+00	-1.481	0.1386
16:00 pm	-1.780e+00	1.280e+00	-1.390	0.1644
17:00 pm	-2.649e+00	1.278e+00	-2.072	0.0383 *
18:00 pm	-2.657e+00	1.278e+00	-2.079	0.0376 *
19:00 pm	-2.442e+00	1.279e+00	-1.910	0.0562 .
20:00 pm	-2.114e+00	1.277e+00	-1.656	0.0977 .
21:00 pm	-2.873e+00	1.299e+00	-2.212	0.0270 *
22:00 pm	-2.462e+00	1.319e+00	-1.866	0.0620 .
23:00 pm	-1.627e+00	1.447e+00	-1.124	0.2609
Oversaturation	1.139e+00	1.183e+00	0.962	0.3359
Long vehicle	-4.165e-01	3.435e-01	-1.212	0.2253
Occ_1	-1.437e-01	1.661e-01	-0.865	0.3868
Occ_2	-7.585e-03	1.352e-01	-0.056	0.9553

Occ_3	-5.209e-02	1.316e-01	-0.396	0.6922
Signif. codes:	0 ‘***’ 0.001 ‘**’ 0.01 ‘*’ 0.05 ‘.’ 0.1 ‘ ’ 1			

2.6.3 Predicting Stop-or-Go Behavior

The non-significant factors are then removed from the original model to form a reduced model and its coefficients are listed in **Table 2. 5**. The reduced model will be used for prediction.

Table 2. 5 Coefficients of logistic regression for the reduced model

Coefficients	Estimate	Std. Error	Z value	Pr(>|z|)
(Intercept)	-2.706e+00	1.337e+00	-2.023	0.0430 *
Signal Phase	-1.446e+00	5.158e-02	-28.039	<2e-16 ***
Speed	8.248e-02	5.237e-03	15.749	<2e-16 ***
Headway	-1.528e-02	2.462e-03	-6.205	5.46e-10 ***
Occ_{max}	-5.072e-01	1.223e-01	-4.148	3.36e-05 ***
Traffic Volume	4.131e-04	1.861e-04	2.220	0.0264 *
13:00 pm	-2.571e+00	1.280e+00	-2.009	0.0445 *
17:00 pm	-2.633e+00	1.283e+00	-2.052	0.0402 *
18:00 pm	-2.639e+00	1.282e+00	-2.058	0.0396 *
21:00 pm	-2.870e+00	1.303e+00	-2.202	0.0276 *
Signif. codes:	0 ‘***’ 0.001 ‘**’ 0.01 ‘*’ 0.05 ‘.’ 0.1 ‘ ’ 1			

Before making prediction, the optimal cut-off probability value needs to be picked from the ROC (Receiver Operating Characteristic) curve in R (shown in **Figure 2. 10**).

The optimal cut-off probability value is 0.665, which maximizes sensitivity and minimizes specificity. Define

$$\hat{p} = \frac{exp(\beta_0+\beta_1 YellowPhase+\beta_2 Speed+\beta_3 Headway+\beta_4 \log(Occ_{max})+\beta_5 Flow+\beta_6 Hour)}{1-exp(\beta_0+\beta_1 YellowPhase+\beta_2 Speed+\beta_3 Headway+\beta_4 \log(Occ_{max})+\beta_5 Flow+\beta_6 Hour)} \quad (6)$$

An event belongs to "go" if $\hat{p} > 0.665$ and "stop" otherwise.

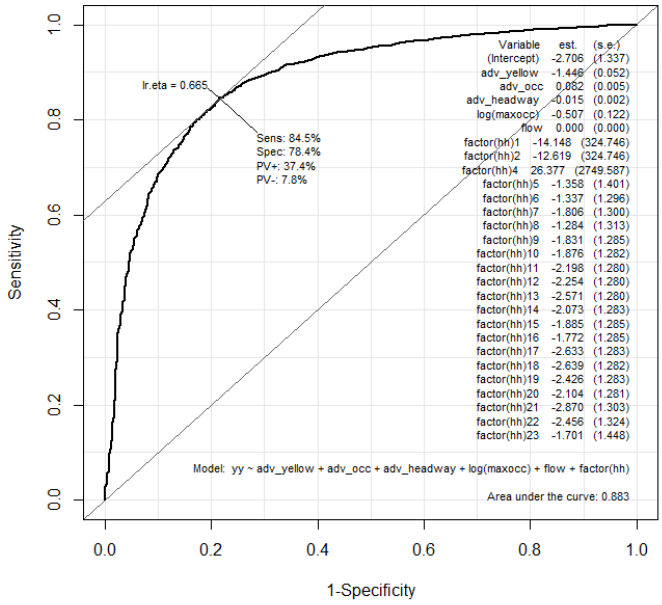

Figure 2. 10 ROC (Receiver Operating Characteristic) curve in R

The prediction accuracy is 83.12%. **Table 2. 6** gives the confusion matrix for prediction:

Table 2. 6 Confusion matrix for prediction result

	prediction		
observation	0	1	Row Total
0	382	137	519

1	233	1440	1673
Column Total	615	1577	2192

CHAPTER 3: IDENTIFYING CROSSING CONFLICT ADVANCE DETECTORS

At a signalized intersection, red light running may incur crossing conflicts, which will likely lead to right-angle crashes. Accordingly, crossing conflicts can be employed as a surrogate for signalized intersection safety evaluation. In chapter 3, we will develop a cost-effective way of predicting crossing conflicts using high-resolution traffic signal data collected from the SMART-Signal systems.

3.1 METHODOLOGY

The stop-or-go prediction model presented in chapter 2 predicts whether a vehicle stops or goes in face of red phase. If it crosses the intersection during the red phase, we will then check whether there is any vehicle coming from the minor road during that time interval. If yes, a potential crossing conflict will be identified. Therefore identifying crossing conflict events includes two steps: (1) identifying "go" events during the red phase on both main and minor roads, and (2) calculating crossing conflicts within conflict zones. The flowchart of these two steps is illustrated in **Figure 3. 1**.

We first briefly describe a process to predict vehicle's stop-or-go behavior, using the event based traffic data. Based on actuation event at an advance detector, the process will predict whether the vehicle will stop or go at the downstream stop bar. Here, we will only focus on those "go" vehicles, which may incur crossing conflicts.

As an initial screening, we first calculate each vehicle's arrival time to an intersection by assuming that it travels at a constant speed and does not change lanes. So the arrival time equals to the distance between advance detector and stop-bar detector divided by its speed at advance detector. Define a time window: $[T_R - Y, T_R + Y]$, where T_R is the red phase start timestamp and Y is the yellow phase duration, i.e., 5.5 second, rounding up to the integer. If the arrival time at the stop bar is within the time window, the event is identified as a potential "go" event. This event will be further checked by applying a "stop or go" model in the next step.

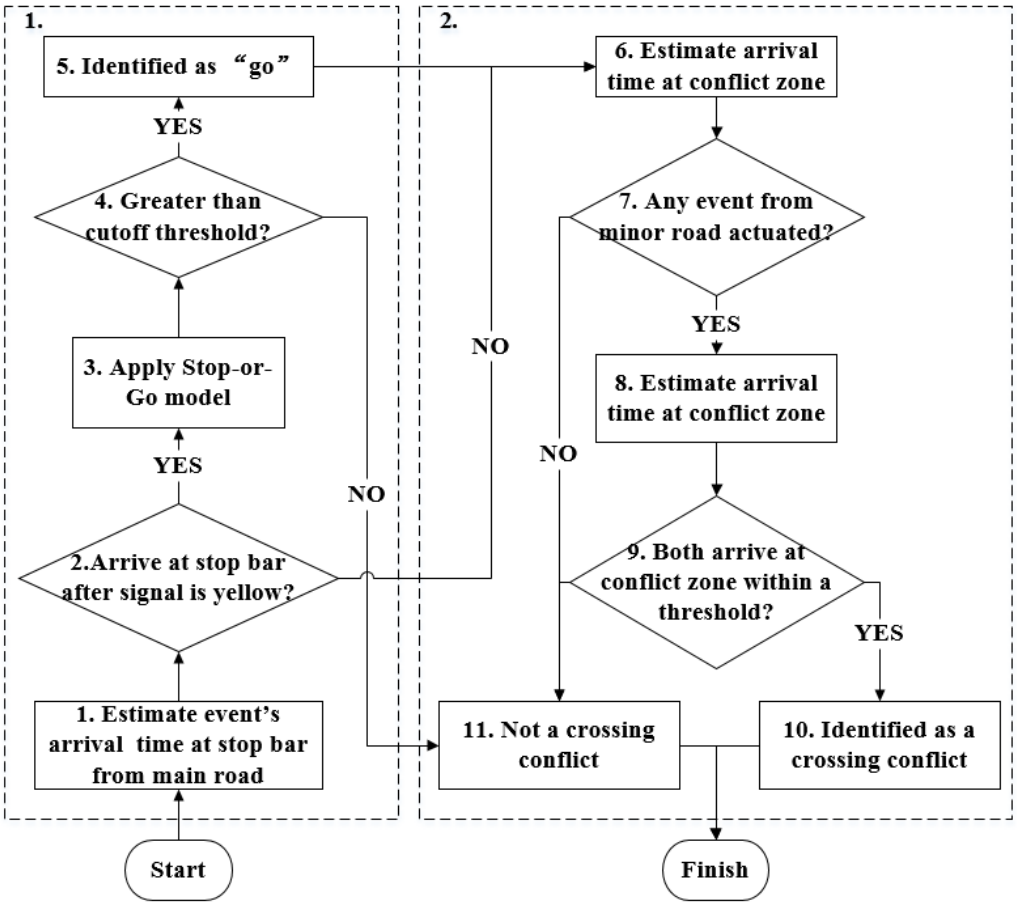

Figure 3. 1 Flowchart of identifying crossing conflict

3.2 STOP-OR-GO BEHAVIOR PREDICTION

A vehicle may not keep a constant speed while approaching an intersection, due to complex traffic conditions and the impact of neighboring vehicles. Therefore, a more complicated model should be employed to refine the initial screening. Here we use the stop-or-go model developed in Chapter 2 to better predict whether one vehicle stops at intersection or crosses the intersection in the form of a logistic regression. To estimate coefficients of a logistic regression model, we first train it using SMART-Signal data from one advance detector at one intersection along TH55 (i.e., training) and then apply the trained model to a comparable intersection sharing similar traffic volumes and same location of advantage detector (i.e., prediction). Information collected from the advance detector includes the passing vehicle's speed or occupancy, the time headway from its leading vehicle, whether this vehicle is a long vehicle or not, traffic volume during that cycle, whether there is oversaturation from downstream traffic, and traffic signal phase status. After removing statistically insignificant factors, the trained logistic regression model includes three significant factors: the signal phase status, vehicle's speed, and its headway from the

leading vehicle. The phase status is defined in Equation 2. With the trained model, the probability of "go" is calculated by Equation 7:

$$P(go) = \hat{p} = \frac{exp(\beta_0+\beta_1 PhaseStatus+\beta_2 Speed+\beta_3 Headway)}{1+exp(\beta_0+\beta_1 PhaseStatus+\beta_2 Speed+\beta_3 Headway)} \quad (7)$$

Where p is the predicted probability of "go" and β is regression coefficients using data collected from TH55 during September 2008-September 2009. If the probability of going is greater than an optimal cut-off value, it is identified as a "go" event. **Table 3. 1** illustrates the availability of SMART-signal data.

Table 3. 1 SMART signal data

Intersection Index	Intersection name	Available date
1	Portland Ave./TH13	2012-2015
2.	W. River Hills Dr./TH13	2012-2015
3.	Cliff Rd./TH13	2012-2015
4.	Rockford Rd./TH55	2015
5.	Industrial Park Blvd./TH55	2015
6.	Medicine Lake Dr./TH55	2015
7.	Winnetka Ave./TH55	2009
		2013-2015
8.	Rhode Island Ave. N/TH55	2009
		2013-2015
9.	Glenwood Ave./TH55	2009
		2013-2015

3.3 CROSSING CONFLICTS IDENTIFICATION WITHIN CONFLICT ZONES

To identify crossing conflicts, we first divide one intersection into four conflict zones (see **Figure 3. 2**). When two vehicles coming from main and minor roads fall within the same conflict zone at the same time, a crossing conflict is identified.

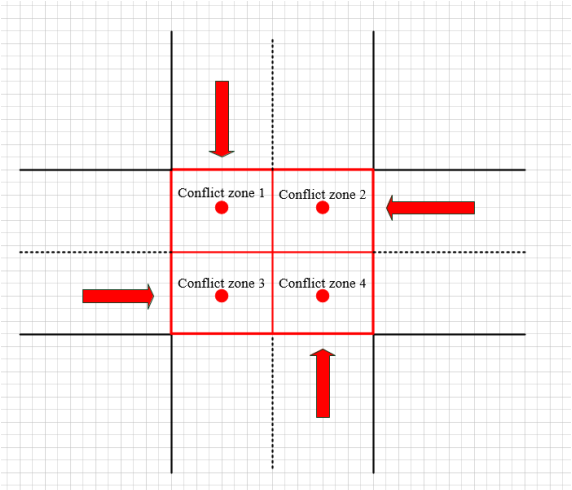

Figure 3. 2 Splitting conflict zones

First, we need to estimate two vehicles' arrival time to each zone. If one vehicle coming from the main road is identified as a "go" vehicle, its arrival time in the desired zone is computed using Equation 8:

$$AT_{main} = T_a + d_x/v, \tag{8}$$

where AT_{main} is the vehicle's arrival time at the desired conflict zone from the main road, T_a is the timestamp when the vehicle arrives at the advance detector on the main street, d_x is the distance to the desired conflict zone from the advance detector, and v is the vehicle speed passing the advance detector.

After the arrival time of the vehicle from the main road is calculated, we will trace all the actuations at the stop-bar detector of the minor road by searching a timestamp window around AT_{main}. A timestamp window for an event leaving the stop-bar detector on minor road is defined as: $[AT_{main} + 7, AT_{main} - 7]$. We choose 7 seconds here because this is the possibly longest travel time for a vehicle on the minor road to travel from the stop bar to the desired conflict zone. The events from the minor road falling within the time window have a high probability of conflicting with the "go" event on the main road.

These events' arrival time at the desired conflict zone can be estimated using its timestamp when they leave the stop bar, given that all minor roads are installed with stop-bar detectors. Since vehicles on the minor road should stand still during the red phase, we assume that they keep a constant acceleration rate to start discharging when the signal phase turns to green. The average speed between when the vehicle leaves the stop-bar detector and arrives at the desired conflict zone, denoted as $\bar{v}$, can be estimated as the average value of speed on the stop-bar detector and speed limit on that approach. Accordingly, arrival time for the vehicle on the minor road at the desired conflict zone is estimated using Equation 9:

$$AT_{minor} = T_s + Occ_s + d_y/\bar{v}, \tag{9}$$

where AT_{minor} is the vehicle's arrival time at the desired conflict zone from the minor road, T_s is the timestamp when the vehicle arrives at the stop-bar detector on the minor road, Occ_s is the occupancy

time, d_y is the distance between the stop-bar detector and the desired conflict zone, and $\bar{v}$ is the average speed.

The crossing conflicts can then be estimated by comparing the arrival times of two vehicles from main and minor roads at the desired conflict zone. If the difference of their arrival time is within a predefined threshold, a crossing conflict is identified. We should note that that a choice of a PET is a tradeoff between accuracy and precision of conflict frequency estimates. A large PET threshold will result in counting many PETs and this will not reflect the severity of conflicts. A short PET threshold produces lower PET counts and lower estimation precision. A PET threshold of 6.5 seconds was found to be a rational choice in Songchitruksa et al.'s study, i.e., $|AT_{minor} - AT_{main}| \leq 6.5$.

3.4 EXAMPLE ILLUSTRATION

In this part, we will use one crossing conflict to illustrate our algorithm step by step. **Figure 3. 3** shows the identified crossing conflict at the intersection of Industrial Park Blvd. /TH55.

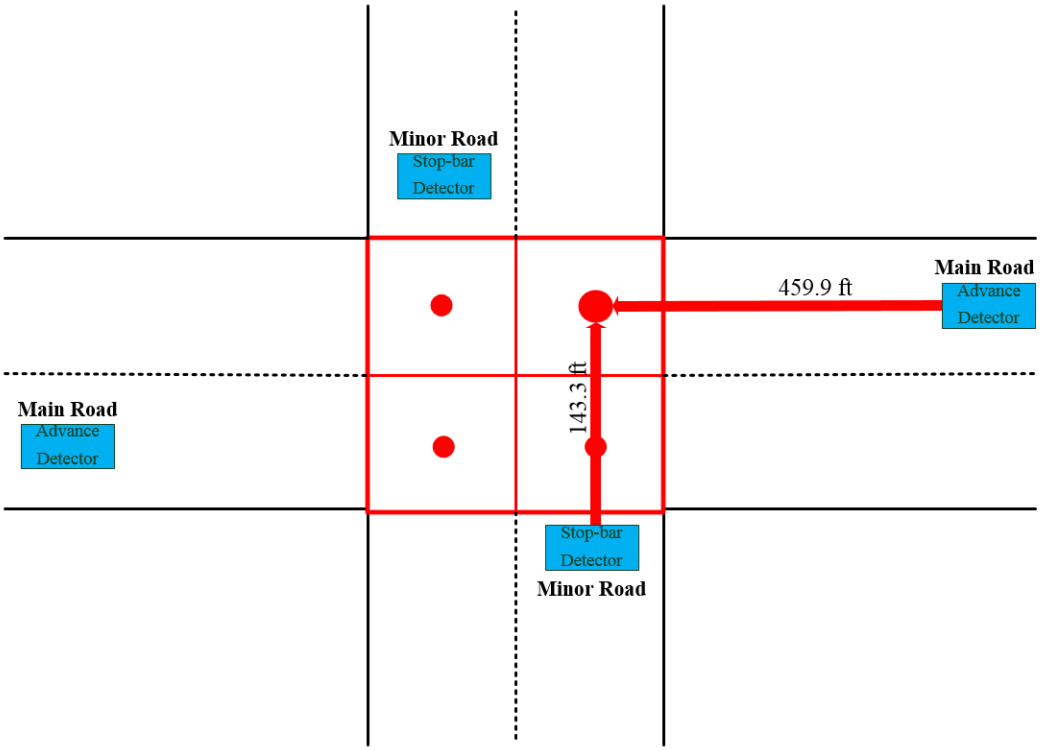

Figure 3. 3 Illustration of the identified crossing conflict

Step 1

First, we search all actuation events at the advance detector. **Table 3. 2** illustrates the raw event record extracted from the advance detector in the database.

Table 3. 2 Advance detector event record in the database

Timestamp	Occupancy (s)	Detector Number
20150507141150300	0.3	7

After transformation, this event actuated the advance detector at 2:11:50 PM. The estimated arrival time at the stop bar is then computed as $2{:}\,11{:}\,50\ \text{PM} + \frac{425(ft)}{25ft/0.3s} = 2{:}\,11{:}\,55\ \text{PM}$.

Step 2

Table 3. 3 shows the original signal phase start timestamp in the database, which corresponds to 2:11:58 PM. As the actuation at 2:11:56 PM happened within the time window of [2:11:58 PM-6s, 2:11:58 PM+6s], i.e., [2:11:52 PM, 2:12:04 PM], based on the initial screening, this could be a "go" event.

Table 3. 3 Signal phase event record in the database

Timestamp	Duration (s)	Phase Number	Phase Status
20150507141157900	15.5	6	Red

Step 3

Given it is a potentially "go" event in the initial screening, we then apply the stop-or-go model to further check the probability of "go" by using Equation 7. **Table 3. 4** illustrates the coefficients of the stop-or-go model estimated from the training data, i.e., information extracted from the intersection Boone Ave. /TH55 from May to September in the year of 2009. The inputs to the model includes signal phase, speed, and headway, they were explained in Chapter 2.

Table 3. 4 Coefficients of the stop-or-go model

Coefficients	Estimate	Std. Error	Z value	Pr(>|z|)
Constant (β_0)	-2.5250337	0.1276932	-19.774	< 2e-16 ***
Signal Phase(β_1)	-1.1151530	0.0117002	-95.311	< 2e-16 ***
Speed (β_2)	0.0130473	0.0015997	8.156	3.47e-16 ***
Headway (β_3)	0.0002176	0.0016206	0.134	0.893
Signif. codes:	0 '***' 0.001 '**' 0.01 '*' 0.05 '.' 0.1 ' ' 1			

The probability of crossing the intersection is calculated by Equation 10:

$$\hat{p} = \frac{exp(-2.525-1.115\ PhaseStatus+0.013Speed+0.0002Headway)}{1+exp(-2.525-1.115\ PhaseStatus+0.013Speed+0.0002Headway)} = 0.71 \quad (10)$$

Step 4

To maximize sensitivity and minimize specificity, an optimal cut-off probability value needs to be picked from the ROC (Receiver Operating Characteristic) curve. This value is chosen in R as **Figure 3. 4** shows. From the ROC curve we can see that the optimal cut-off probability value is 0.431.

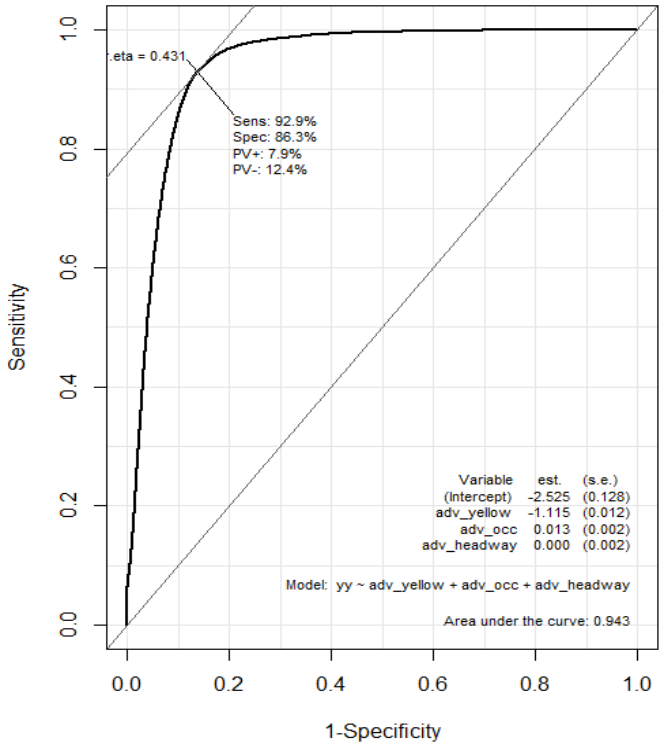

Figure 3. 4 ROC (Receiver Operating Characteristic) curve in R

Step 5

Figure 3. 4 illustrated the optimal cutoff threshold which is trained by our training dataset. If the probability is greater than cutoff threshold, it is considered as a "go" event, otherwise it is a "stop" event. The estimated "go" probability for this vehicle is 0.71 which is greater than the cutoff threshold 0.431, thus this event is determined as a "go" event.

Step 6

For this "go" event, the arrival time from the major road at desired conflict zone is calculated by Equation 8 as $AT_{main} = 2{:}11{:}50\ \text{PM} + \frac{459.9\ (ft)}{\frac{25ft}{0.3}} = 2{:}11{:}56\ \text{PM}.$

Step 7

We need to check if there is a vehicle coming from the minor road and arrive at the desired conflict zone at the same time. By checking the stop bar detector on the minor road, one actuation record is found (shown in

Table 3. 5). This event actuates the stop-bar detector #14 at 2:11:47 PM with an occupancy of 2.7 second.

Table 3. 5 Stop-bar detector event record in the database

Timestamp	Occupancy (s)	Detector Number
20150507141147100	2.7	14

Step 8

The arrival time of the vehicle from the minor road at desired conflict zone is calculated by Equation 9 as $AT_{minor} = 2{:}11{:}47 \text{ PM} + 2.7s + \frac{143.3\ (ft)}{\frac{25ft}{2.7s} + 51.33\text{ft/s}} = 2{:}11{:}55 \text{ PM}$, where 51.33 ft/s is the speed limit on the minor road.

Step 9

The arrival time of two identified events at the desired conflict zone from the main road and minor road are 2:11:56 PM and 2:11:55 PM, respectively. The arrival time difference is 1s which is smaller than the threshold 6.5 s.

Step 10

So we identify it as one crossing conflict. This concludes our algorithm of identifying a crossing conflict.

3.5 CROSSING CONFLICTS SUMMARY

Using the proposed algorithm, we estimated daily crossing conflicts at each intersection for each year. The result is shown in **Table 3. 6**. As we can see from the result, the number of daily crossing conflicts varied across different intersections, mainly from 7.9 to 51.2. The cases highlighted in red were involved with relatively more crossing conflicts than the others. This could indicate a higher risk of right-angle collisions at those intersections, and comprehensive safety evaluation may be needed.

Table 3. 6 Estimated crossing conflicts

NO.	Intersection name	Year	Daily crossing conflicts
1	Portland Ave./TH13	2012	40.5
		2013	16.2
		2014	47.5
		2015	46.2

2.	W. River Hills Dr./TH13	2012	44.6
		2013	41.8
		2014	46.2
		2015	37.1
3.	Cliff Rd./TH13	2012	31.4
		2013	29.2
		2014	36.2
		2015	39.6
4.	Rockford Rd./TH55	2015	20.6
5.	Industrial Park Blvd./TH55	2015	49.7
6.	Medicine Lake Dr./TH55	2015	48.4
7.	Winnetka Ave./TH55	2009	38.6
		2013	51.2
		2014	15.8
		2015	47.1
8.	Rhode Island Ave. N/TH55	2009	10.1
		2013	13.0
		2014	11.3
		2015	12.8
9.	Glenwood Ave./TH55	2009	7.9
		2013	9.8
		2014	11.7
		2015	13.1

CHAPTER 4: RIGHT-ANGLE CRASH MODEL REGRESSION

An important working hypothesis for this research is that the frequency of crossing conflicts at an intersection could be a reliable indicator of the risk for angle crashes. The idea that non-crash events might be reliable indicators of crash events dates back to at least to Perkins and Harris (1968), while recently there has been an emphasis on using traffic conflicts generated in microsimulation programs as predictors of crash risk (Gettman and Head 2003; Archer and Young 2010). As the *Highway Safety Manual* (AASHTO 2010) (HSM) documents, however, the most reliable predictor of crash frequency is traffic volume and one might expect that as traffic volume increases both conflict and crash frequencies would also increase. A demonstrated correlation between conflict frequency and crash frequency could then be due to conflict frequency acting as a surrogate for traffic volume rather than being an indicator of crash risk. To test this hypothesis it is necessary to include measures of both traffic volume and conflict frequency in statistical models that attempt to predict crash frequency. This chapter describes an initial effort at conducting such a test. Crash records and average daily traffic data were collected for seven four-legged SMART-SIGNAL intersections and then the methods described in Chapter 3 were used to compute estimates of the frequency of crossing conflicts at these intersections. Several versions of a safety performance function (SPF) similar to that used in the *Highway Safety Manual* were then evaluated to see if average crossing-conflict frequency could reliably predict the frequency of angle crashes after controlling for traffic volume.

4.1 DATA PREPARATION

The first step was to identify intersections where SMART-SIGNAL data were available. A review of SMART-SIGNAL deployments identified nine intersections, seven four-legged intersections and two T-intersections. These are listed in **Table 4. 1**.

Table 4. 1 Intersections with SMART-SIGNAL Data

Major Road	Minor Road	Type
MNTH 13	Portland Ave	4-legged
MNTH 13	West River Hills Drive	4-legged
MNTH 13	Cliff Road	4-legged
MNTH 55	Rockford Road	4-legged
MNTH 55	Industrial Park Blvd	4-legged

MNTH 55	Medicine Lake Road	4-legged
MNTH 55	Winnetka Ave	4-legged
MNTH 55	Rhode Island Ave	T-intersection
MNTH 55	Glenwood Ave	T-intersection

The next step was to compile crash and annual average daily traffic (AADT) data for each of the candidate intersections. Because 4-legged and T intersections can differ as to their crash-generating tendencies attention was restricted to the seven 4-legged intersections listed in **Table 4. 1**. Using MNCMAT, crash records were extracted for each of the intersections and for all available years, 2005-2015. The crash records contained information on the year the crash occurred and also a characterization of the "Vehicular relationship that led to the crash" in the DIAGRAM field. The DIAGRAM code for an angle crash is 05, and for each intersection and for each year a count of the DIAGRAM 05 crashes was made. The annual totals of reported angle crashes ranged from 0 to 4. Data provided on MnDOT's Traffic Analysis and Forecasting website were then used to compile AADTs for the SMART-SIGNAL intersections. AADT values for each leg of each intersection, and for each year from 2005-2015, were recorded and then, following the procedure recommended in the *Highway Safety Manual*, the larger of the two-way volumes, for the major and the minor approaches, were added to the data file. Finally, using the method described in Chapter 3, estimated daily crossing conflicts were computed at each intersection and for each year when SMART-SIGNAL data were available. These data are listed in the Appendix.

4.2 STATISTICAL ANALYSES

Key components of the prediction methodology developed in the HSM are the safety performance functions which relate the expected annual frequency of crashes at a location to traffic volumes and, in some cases, other measurable features. For signalized intersections on urban and suburban arterials the SPF for multiple-vehicle crashes is given by

$$N = \exp\left(-10.99 + (1.07)\ln(AADT_{Major}) + (0.23)\ln(AADT_{Minor})\right) \quad (11)$$

Where N is expected multiple-vehicle crashes/year,

exp(.) denotes the exponential function,

AADT_{Major} denotes Major approach annual average daily traffic,

AADT_{Minor} denotes Minor approach annual average daily traffic,

ln(.) denotes the natural logarithm function.

For example, at an intersection where the AADT on both the Major and Minor approaches was 1.0 vehicles/day, the expected crash frequency would be exp(-10.99)=0.000017 crashes/year. A 1% increase in Major approach AADT leads to a 1.07% increase in predicted crash frequency while a 1% increase in Minor approach AADT leads to a 0.23% increase in predicted crash frequency. At an intersection with a Major AADT of 10,000 vehicles/day and a Minor AADT of 2000 vehicles/day the predicted crash frequency is

$$\exp\left(-10.99+(1.07)\ln(10000)+(0.23)\ln(2000)\right)=1.85\ crashes/year$$

The HSM also notes that typically about 25% of multi-vehicle crashes are angle crashes.

As a first step it was decided to fit a similar SPF for angle crashes at the seven four-legged SMART-SIGNAL intersections using all available crash and AADT data. Annual crash counts were treated as independent Poisson outcomes with expected values following the SPF

$$N=\exp\left(\beta_1+(\beta_2)\ln(AADT_{Major})+(\beta_3)\ln(AADT_{Minor})\right) \quad (12)$$

As in the above example the coefficient β_1 in equation (12) is related to the expected crash frequency when traffic volumes are minimal while the coefficients β_2 and β_3 give the predicted increases in crash frequency associated with 1% increases in Major and Minor approach traffic volumes. A value $\beta_2=0$ means that changes in Major approach AADT have no effect on predicted crash frequency while a value of $\beta_3=0$ means Minor approach AADT has no effect on crash frequency.

Maximum likelihood estimates of the coefficients β_1, β_2, and β_3 appearing in equation (12) were computed using Mathcad's (Maxfield 2009) nonlinear equation solver, while statistical inference was based on standard results for generalized linear models (Dobson and Barnett 2008). **Table 4. 2** summarizes the results for this exercise.

Table 4. 2 Results from Fitting Model with Major and Minor AADT as Angle-Crash Predictors

Variable (coefficient)	Estimate	Std. Error	Z value	P-value
$Constant$ (β_1)	-10.59	6.57	-1.61	0.1
$ln(AADT_{Major})$ (β_2)	0.51	0.63	0.80	0.42
$ln(AADT_{Minor})$ (β_3)	0.54	0.09	5.87	< .001

The Estimate column in **Table 4. 2** lists the estimated coefficient while the Std. Error column lists the associated standard errors. The Z-value column lists tests of whether or not the associated coefficients can be taken to equal zero, that is, whether or not the AADTs help predict crash frequency. The P-value column gives probabilities of obtaining the test statistics if the coefficients equaled zero. The results summarized in **Table 4. 2** indicate that, at these intersections, Minor AADT is a reliable predictor of angle-

crash frequency (the coefficient β_3 is significantly different from zero) but that the Major AADT coefficient β_2 is not significantly different from zero. That is, knowledge of Major AADT does not help predict angle-crash frequency. This finding is confirmed by using the likelihood-ratio test to compare equation (12) to a simpler model having only the constant term and Minor AADT as predictors. The computed Chi-squared statistic was 0.384, with one degree-of-freedom and a p-value of 0.464, indicating that an SPF without Major AADT and one with Major AADT provided essentially equivalent descriptions of how the crash frequencies varied. The failure of Major AADT to help predict crash frequency is probably due the fact that the intersections were neighbors along two trunk highways so that the Major approach AADTs showed little site-to-site variation.

The next set of analyses looked to see if adding a measure of crossing conflicts improved the ability to predict angle crashes. *Since SMART-SIGNAL data were available for at most four years these analyses were based on a limited crash experience (11 crashes total) and so should be regarded as preliminary.*

A model similar to equation (12), but with the natural logarithms of the minor approach AADTs and of the estimated average crossing conflicts, was fit using maximum likelihood and the results are shown in **Table 4. 3**.

Table 4. 3 Results from Fitting a Model with Minor AADT and Red-Light Running Frequency as Angle Crash Predictors

Variable	Estimate	Std. Error	Z value	P-value
$\boldsymbol{Constant}$	-13.49	1.36	-9.92	<.001
$\boldsymbol{ln(AADT_{Minor})}$	0.31	0.14	2.30	0.02
$\boldsymbol{ln(Crossing\ Conflicts)}$	2.73	0.26	10.47	< .001

Table 4. 3 suggests that both Minor AADT and estimated average crossing conflicts help predict angle-crash crash frequency (all p-values are less than 0.05) and that the crossing conflict frequency might be a more important predictor. This was confirmed by comparing the two-predictor model summarized in **Table 4. 3** to a model having only average crossing conflicts as a predictor, using the likelihood ratio test. The computed Chi-squared statistic was 0.56, $p = 0.55$ with one degree of freedom. That is, at least for this limited data set, a model with only crossing conflicts as its predictor was almost as good as one with crossing conflicts and Minor AADT.

Finally, although the details are not described here, adding Major AADT produced no improvement over the simpler models that included average crossing conflicts.

CHAPTER 5: CONCLUSION

In this project, we developed two methodologies for intersection safety evaluation using high-resolution traffic signal data collected from the SMART-Signal system: red-light running (RLR) for those with stop-bar and entrance detectors; and crossing conflicts for those with only advance detectors, based on our work on stop-or-go prediction modeling.

Then we tested whether adding a measure of red-light running to a more standard model containing AADTs could improve the ability to predict angle crashes at signalized intersections. Although any conclusion should be regarded as preliminary, due to the limited data available, for these data, it appears that the crossing conflict measures are superior to either major approach AADT or minor approach AADT as a predictor of angle-crash frequency.

In the future, the work proposed in this project may be extended in two directions. First, we may improve the prediction accuracy of the developed model when more data collected from the SMART-SIGNAL system becomes available. Second, video cameras can be installed at intersections to validate our proposed methodologies.

REFERENCES

Abbas, M., Machiani, S. G., Garvey, P. M., Farkas, A., and Lord-Attivor, R. (2014). Modeling the Dynamics of Driver's Dilemma Zone Perception Using Machine Learning Methods for Safer Intersection Control (No. MAUTC-2012-04).

Abdel-Aty, M., Lee, C., Wang, X., Nawathe, P., Keller, J., Kowdla, S., and Prasad, H. (2006). Identification of Intersections' Crash Profiles/Patterns.

Amundson, F.H., and Hyden, C., (1977). Proceedings of the First Workshop on Traffic Conflict, Institution of Transport Economics, Lind Institute of Technology, Oslo, Norway.

Archer, J., (2005). Indicators for traffic safety assessment and prediction and their application in micro-simulation modelling: a study of urban and suburban inter-sections. In: Doctoral Dissertation. Department of Infrastructure, Division for Transport and Logistic (TOL), Centre for Transport Research, Royal Institute of Technology, Stockholm, Sweden.

AASHTO, Highway Safety Manual, American Association of State Highway and Transportation Officials, (2010).

Archer, J., and Young, W. (2010, January). A traffic microsimulation approach to estimate safety at unsignalised intersections. In Transportation Research Board Annual Meeting, 89th, 2010, Washington, DC, USA (No. 10-0683).

Bonneson, J., and Son, H. (2003). Prediction of expected red-light-running frequency at urban intersections. Transportation Research Record: Journal of the Transportation Research Board, (1830), 38-47.

Chatterjee, I., and Davis, G. A. (2011). Can High-Resolution Detector and Signal Data Support Intersection Crash Identification and Reconstruction? In 3rd International Conference on Road Safety and Simulation.

Dobson, A., and Barnett, A., An Introduction to Generalized Linear Models, third edition, CRC Press, 2008.

Elmitiny, N., Yan, X., Radwan, E., Russo, C., and Nashar, D. (2010). Classification analysis of driver's stop/go decision and red-light running violation. Accident Analysis and Prevention, 42(1), 101-111.

Gates, T., Noyce, D., Laracuente, L., and Nordheim, E. (2007). Analysis of driver behavior in dilemma zones at signalized intersections. Transportation Research Record: Journal of the Transportation Research Board, (2030), 29-39.

Gettman, D., and Head, L. (2003). Surrogate safety measures from traffic simulation models. Transportation Research Record: Journal of the Transportation Research Board, (1840), 104-115.

Liu, Y., Chang, G. L., Tao, R., Hicks, T., and Tabacek, E. (2007). Empirical observations of dynamic dilemma zones at signalized intersections. Transportation Research Record: Journal of the Transportation Research Board, (2035), 122-133.

Liu, H. X., Wu, X., Ma, W., and Hu, H. (2009). Real-time queue length estimation for congested signalized intersections. Transportation research part C: emerging technologies, 17(4), 412-427.

Maxfield, B. (2009). Essential Mathcad for Engineering, Science, and Math W/CD. Academic Press.

Mitra, S., Chin, H. C., and Quddus, M. (2002). Study of intersection accidents by maneuver type. Transportation Research Record: Journal of the Transportation Research Board, (1784), 43-50.

Perkins, S. R., and Harris, J. L. (1968). Traffic conflict characteristics-accident potential at intersections. Highway Research Record, (225).

Poch, M., and Mannering, F. (1996). Negative binomial analysis of intersection-accident frequencies. Journal of transportation engineering, 122(2), 105-113.

Porter, B. E., and Berry, T. D. (2001). A nationwide survey of self-reported red light running: measuring prevalence, predictors, and perceived consequences. Accident Analysis and Prevention, 33(6), 735-741.

Porter, B. E., and England, K. J. (2000). Predicting red-light running behavior: a traffic safety study in three urban settings. Journal of Safety Research, 31(1), 1-8.

Papaioannou, P. (2007). Driver behaviour, dilemma zone and safety effects at urban signalised intersections in Greece. Accident Analysis and Prevention, 39(1), 147-158.

Perkins, S. R., and Harris, J. L. (1968). Traffic conflict characteristics-accident potential at intersections. Highway Research Record, (225).

Rakha, H., and El-Shawarby, I., and Setti, J.R., (2007). Characterizing driver behavior on signalized intersection approaches at the onset of a yellow-phase trigger. IEEE Transactions on Intelligent Transportation Systems, 8(4): 630-640.

Retting, R., Williams, A., and Greene, M. (1998). Red-light running and sensible countermeasures: Summary of research findings. Transportation Research Record: Journal of the Transportation Research Board, (1640), 23-26.

Sharma, A., Bullock, D. and Peeta, S., (2011). Estimating dilemma zone hazard function at high-speed isolated intersection. Transportation research part C. 19 (3): 400—412

Songchitruksa, P., and Tarko, A. (2006). Practical method for estimating frequency of right-angle collisions at traffic signals. Transportation Research Record: Journal of the Transportation Research Board, (1953), 89-97.

Sayed, T., Brown, G., and Navin, F. (1994). Simulation of traffic conflicts at unsignalized intersections with TSC-Sim. Accident Analysis and Prevention, 26(5), 593-607.

Songchitruksa, P., and Tarko, A. (2006). Practical method for estimating frequency of right-angle collisions at traffic signals. Transportation Research Record: Journal of the Transportation Research Board, (1953), 89-97.

Wu, X., Vall, N., Liu, H., Cheng, W., and Jia, X. (2013). Analysis of drivers' stop-or-run behavior at signalized intersections with high-resolution traffic and signal event data. Transportation Research Record: Journal of the Transportation Research Board, (2365), 99-108.

Yang, C. D., and Najm, W. G. (2007). Examining driver behavior using data gathered from red light photo enforcement cameras. Journal of safety research, 38(3), 311-321.

Zhang, L., Zhou, K., Zhang, W. B., and Misener, J. (2009). Prediction of red light running based on statistics of discrete point sensors. Transportation Research Record: Journal of the Transportation Research Board, (2128), 132-142.

APPENDIX A: DATA USED IN CRASH PREDICTION ANALYSES

Intersection	Year	Angle Crashes	Minor AADT	Major AADT	Average Crossing Conflicts
Portland Ave./TH13	2005	0	3000	31500	NA
	2006	1	3000	29500	NA
	2007	0	3200	29500	NA
	2008	1	3200	29000	NA
	2009	0	3200	29000	NA
	2010	1	3400	30000	NA
	2011	0	3400	30000	NA
	2012	0	3400	30500	40.5
	2013	0	3400	30500	16.15
	2014	2	3250	30500	47.47
	2015	0	3250	29500	46.2
W. River Hills Dr./TH13	2005	1	10800	28000	NA
	2006	1	10500	28500	NA
	2007	1	9800	28500	NA
	2008	0	9800	28500	NA
	2009	0	9800	28500	NA
	2010	0	9800	28000	NA
	2011	1	9500	28000	NA

	2012	0	9500	28000	44.56
	2013	0	10900	28000	41.76
	2014	2	10900	27000	46.2
	2015	0	10400	28500	37.1
Cliff Rd./TH13	2005	4	28000	25000	NA
	2006	1	28500	25000	NA
	2007	0	28500	25000	NA
	2008	1	28500	25500	NA
	2009	1	28500	25500	NA
	2010	2	28000	24700	NA
	2011	1	28000	20200	NA
	2012	0	28000	18900	31.37
	2013	0	28000	18900	29.19
	2014	1	27000	18900	36.2
	2015	1	28500	21800	39.55
Rockford Rd./TH55	2005	1	17500	33000	NA
	2006	1	17500	32000	NA
	2007	0	18300	32000	NA
	2008	0	18300	33500	NA

	2009	2	16600	33500	NA
	2010	0	16600	36000	NA
	2011	0	16200	36000	NA
	2012	4	16200	34000	NA
	2013	1	17000	34000	NA
	2014	1	17000	34000	NA
	2015	1	15800	34000	20.58
Industrial Park Blvd./TH55	2005	0	1750	28000	NA
	2006	0	1750	27000	NA
	2007	0	1750	27000	NA
	2008	0	1750	27500	NA
	2009	0	1900	27500	NA
	2010	1	1900	29000	NA
	2011	0	1900	29000	NA
	2012	1	1900	30500	NA
	2013	0	2200	30500	NA
	2014	1	2200	30500	NA
	2015	1	2200	30500	49.7
Medicine Lake Dr./TH55	2005	0	5400	37000	NA

	2006	1	5400	37000	NA
	2007	0	5900	37000	NA
	2008	0	5900	34000	NA
	2009	0	5500	34000	NA
	2010	1	5500	32000	NA
	2011	0	5500	32000	NA
	2012	0	5500	35000	NA
	2013	1	5400	35000	NA
	2014	0	5400	35000	NA
	2015	0	5400	35000	48.4
Winnetka Ave./TH55	2005	2	15100	40000	NA
	2006	0	15100	34000	NA
	2007	0	14600	34000	NA
	2008	1	14600	35000	NA
	2009	0	14500	35000	38.52
	2010	2	14500	33500	NA
	2011	1	13800	33500	NA
	2012	0	13800	36000	NA
	2013	2	15200	36000	51.2

	2014	0	15200	36000	15.8
	2015	1	15800	36000	47.1